Chinese Physics Letters

EXPRESS LETTER

Spin-Valley Anderson Impurity in Moiré Systems: Phase Diagram, Pairing, and Pseudogap

Cite as: Yi-Jie Wang *et al*. 2026 *Chin. Phys. Lett.* **43** 080708

DOI CSTR

Recommended Articles

Flat Band and η-Pairing States in a One-Dimensional Moiré Hubbard Model
R. Wang, and Z. Song
Chin. Phys. Lett. **41**, (2024)

Nano-Opto-Electro-Mechanical Systems from Moiré Superlattices
Qin-Yang Zeng, Gui-Xin Su, Xin-Yu Mei, Han Wang, Ping-Heng Tan, and Xin Zhang
Chin. Phys. Lett. **43**, 050701 (2026)

Giant Spontaneous Valley Polarization and Adsorption-Induced Topological Phase Transition in Single-Layer 2H-$NbTe_2$
Bo Huang, Shu-Zong Li, Zhixiong Yang, Zhenqing Li, Hongxing Li, and Wei-Bing Zhang
Chin. Phys. Lett. **42**, 067501 (2025)

Interplay of Kitaev Interaction and Off-Diagonal Exchanges: Exotic Phases and Quantum Phase Diagrams
Qiang Luo, Jize Zhao, and Xiaoqun Wang
Chin. Phys. Lett. **42**, 027501 (2025)

Artificial Cooper-Pair Density Modulation in Buckled Heterostructure
Zhongrui Wang *et al*.
Chin. Phys. Lett. **43**, 030707 (2026)

Symmetry Breaking and Phase Transitions in Twisted Rhombohedral Trilayer-Bilayer Graphene
Jingwei Dong *et al*.
Chin. Phys. Lett. **43**, 060716 (2026)

A series journal of Chinese Physical Society distributed by IOP Publishing

Chinese Physics Letters

Chin. Phys. Lett. **43** 080708 (2026)

EXPRESS LETTER

DOI: 10.1088/0256-307X/43/8/080708
CSTR: 32039.14.0256-307X.43.8.080708

Spin-Valley Anderson Impurity in Moiré Systems: Phase Diagram, Pairing, and Pseudogap

Yi-Jie Wang(王一杰)[1,†], Geng-Dong Zhou(周耿栋)[1,†], Hyunsung Jung(정현성)[2], Seongyeon Youn(윤성연)[2,3], Seung-Sup B. Lee(이승섭)[2,3,4,*], and Zhi-Da Song(宋志达)[1,5,6,*]

[1]International Center for Quantum Materials, School of Physics, Peking University, Beijing 100871, China
[2]Department of Physics and Astronomy, Seoul National University, Seoul 08826, Korea
[3]Center for Theoretical Physics, Seoul National University, Seoul 08826, Korea
[4]Institute for Data Innovation in Science, Seoul National University, Seoul 08826, Korea
[5]Hefei National Laboratory, Hefei 230088, China
[6]Collaborative Innovation Center of Quantum Matter, Beijing 100871, China

[†]These authors contributed equally to this work.
[*]Corresponding authors. Email: sslee@snu.ac.kr; songzd@pku.edu.cn

Recent experiments support that the magic-angle graphene family can be modeled by a periodic array of correlated quantum impurities immersed in a Dirac sea. This work *analytically* demonstrates that, with (anti-)Hund's interactions that can originate from electron-phonon couplings, a single impurity can exhibit novel quantum phase transitions, and readily nurture the pairing potential and pseudogap phenomenon relevant to this moiré family. For broad applicability, we tackle a spin-valley Anderson impurity with general symmetry-allowed (anti-)Hund's parameters (J_D, J_S), and derive its full phase diagram at half-filling. While the model reduces to well-known Kondo problems in certain limits, we uncover that in the large J_D regime, the low-energy physics is controlled by a novel "pair-Kondo" coupling between the bath and an impurity valley-doublet. Using bosonization–refermionization mapping, we show there is a BKT transition from a Fermi liquid with pair-Kondo resonance, into an anisotropic doublet phase that exhibits a non-analytic zero-energy kink in the impurity spectral function, and non-universal power-law scaling in impurity susceptibilities. Importantly, by analyzing the pairing potentials across the phase diagram, we unveil ubiquitous existence of attractive channels under general (anti-)Hund's interactions. More crucially, we analytically reveal the pseudogap shoulders represent multiplet excitations induced by the injected electron or hole, and derive ansätze of correlation self-energy that reproduce the pseudogap phenomenon in the lattice. All results are established analytically, with further verification by numerical renormalization group calculations.

Introduction

Moiré hetero-structures have opened up a new stage to engineer electronic flat bands, providing unprecedented possibilities to study exotic correlations besides conventional materials [1−3]. In a variety of systems, flat bands originate from the formation of local orbitals at the moiré length scale [4−10], akin to the atomic d or f shells, but with richer inner degrees of freedom such as layer and valley. More importantly, with an underlying lattice, electrons interact not only through the Coulomb repulsion, but also through microscopic processes such as phonons [11,12], which act non-trivially on the new degrees of freedom. These aspects imply that, even for a model as simple as a local orbital, new physics is yet to be explored.

One paradigmatic moiré material is the magic-angle twisted bilayer/trilayer graphene (MATBG/TTG) [13], where correlated (Chern) insulators [14−22], unconventional superconductivity [14,15,23−36] with pseudogaps [37−39], and strange metal transport [40−42] are discovered. It is then realized that the topological flat bands [43−47] can be disentangled into moiré local orbitals (f) [6−8] hybridizing with itinerant Dirac bands (c) [48−52]. Coulomb repulsion generates a large Hubbard $U \sim 60$ meV on each f orbital, promoting the formation of local moments. Fermi liquid (FL) phases of heavy fermion or mixed-valence types can form via the Kondo screening by the c electrons. Various phenomena get explained within this framework [53−64], including the Pomeranchuk effect [65−67], cascade transitions in scanning tunneling microscope (STM) spectrum [68,69] and compressibility [33,67,70]. The coexistence of correlated f and light c is supported by thermoelectric transport [71] and the quantum twisting microscopy [72]. The Kondo resonance is also recently observed in STM [39].

Intriguingly, in MATBG/TTG, the superconductivity gap coexists with a larger pseudogap [38,39] that appears at an energy scale of 1 meV, comparable to the phonon-mediated electron-electron interaction J [73−80]. In the Hilbert space of an f local moment, J induces anti-Hund's splitting favoring spin-singlet configurations [81−85], in stark contrast to the atomic f shells with a conventional Hund's rule. Based on the assumption that a local FL emerges at energy below $O(J)$, a previous work demonstrates that quasiparticles experience an attractive renormalized interaction [86]. In addition, recent dynamical mean-field theory (DMFT) works also show that J leads to pseudogaps of size $O(J)$ and different quantum phases [87]. These studies strongly indicate that the anti-Hund's splitting can account for both pairing and pseudogap.

In this context, we consider a spin-valley Anderson impurity model (SVAIM) with a general valley-anisotropic (anti-)Hund's interaction, which can also describe a correlated orbital in the hetero-strained MATBG/TTG [88,89]. We study its full phase diagram analytically, with support by numerical renormalization group (NRG) calculations, and analyze the occurrence of pairing and pseudogap. Analytical solutions to the finite-size many-body spectrum and detailed RG flow calculations are provided in a companion work [90].

Model

Hetero-strain in MATBG/TTG lifts the otherwise degenerate orbital angular momenta of f [48] into bonding and anti-bonding levels

Received 26 April 2026; accepted 20 July 2026; published 28 August 2026
© 2026 Chinese Physical Society and IOP Publishing Ltd. All rights, including for text and data mining, AI training, and similar technologies, are reserved.

Check for updates

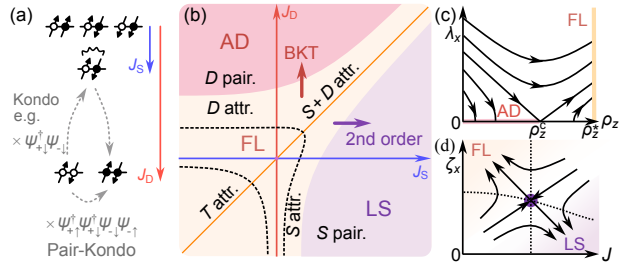

Fig. 1. (a) Two-electron impurity states. White and black circles indicate valleys $l=\pm$, respectively, and arrows indicate spin $s=\uparrow\downarrow$. Equation (1) lowers the energy of the singlet S (the valley doublet D) by J_S (J_D), compared to the spin triplet T. (b) Schematic phase diagram of SVAIM. The FL phase is separated from the AD phase by a BKT transition, and separated from the LS phase by a second-order transition. Dashed lines mark the crossover boundaries within the FL phase, beyond which renormalized interactions turn attractive ("attr.") in certain channels (S, D, or T). AD and LS phases also exhibit enhanced pairing ("pair.") susceptibilities in the corresponding channels, despite no quasiparticle exists. (c) and (d) Schematic RG flows for the BKT and second-order transitions, respectively. For NRG results corresponding to panels (b)–(d), see Supplementary Material [91].

[52], while leaving the valley ($l=\pm$) and spin ($s=\uparrow\downarrow$) symmetries intact. Upon electron (hole) doping, the bonding (anti-bonding) level remains frozen [62,63], thus it suffices to model the active levels with electron operators f_{ls}. We introduce Pauli matrices $[\sigma^\mu]_{l,l'}$ and $[\varsigma^\nu]_{s,s'}$ ($\mu,\nu=0,x,y,z$) for valley and spin, respectively. Besides charge-U(1) symmetry generated by $\sigma^0\varsigma^0$, there are spin-SU(2) symmetry generated by $\varsigma^{x,y,z}$, valley-U(1) symmetry generated by σ^z, and a C_{2z} symmetry that swaps the two valleys represented by σ^x.

The SVAIM is described by $H=H_0+H_{\rm imp}+H_c$. The bath Hamiltonian $H_0=\int \mathrm{d}x\sum_{ls}:\psi^\dagger_{ls}(x)(\mathrm{i}\partial_x)\psi_{ls}(x):$ is chosen as a chiral fermion for the convenience of analytical treatment, $H_c=\sqrt{2\Delta_0}\sum_{ls}f^\dagger_{ls}\psi_{ls}(0)$ is the hybridization between the impurity and bath states, and $H_{\rm imp}=(U/2)(N-2)^2+H_{\rm AH}$ is the impurity Hamiltonian. U is the Hubbard repulsion, N counts the impurity electron number, and $H_{\rm AH}$ is a general symmetry-allowed (anti-)Hund's interaction. By symmetry, the two-electron subspace can split into a spin triplet (T), a valley doublet (D) carrying total valley charges $L^z=2,\bar{2}$, and a singlet (S) [Fig. 1(a)]. Therefore, we parametrize

$$H_{\rm AH}=-\frac{J_S}{2}\sum_{ll'}f^\dagger_{l\uparrow}f^\dagger_{\bar{l}\downarrow}f_{\bar{l}'\downarrow}f_{l'\uparrow}-J_D\sum_l f^\dagger_{l\uparrow}f^\dagger_{l\downarrow}f_{l\downarrow}f_{l\uparrow}, \tag{1}$$

where $\bar{l}$ is the opposite valley to l. $J_{S,D}$ lowers the energy of S,D relative to T, respectively, thus $J_{S,D}>0$ corresponds to an anti-Hund's rule. Since $S\oplus D$ forms the "valley triplet" of a valley-SU(2) group generated by $\sigma^{x,y,z}$, $J_S\neq J_D$ describes valley-anisotropy. As $J_{S,D}$ originate from phonon-mediated interactions [84], they are much weaker than the Coulomb repulsion U [91]. We focus on half-filling where the multiplet splitting can dominate the physics, and utilize the particle-hole symmetry there to simplify analysis. Particle-hole asymmetry will not affect our main conclusions.

At energy $\omega\ll O(U)$, charge fluctuations on f get frozen, turning into virtual processes that induce Kondo couplings, $|\Xi\rangle\langle\Xi'|:\psi^\dagger\sigma^\mu\varsigma^\nu\psi:$ [91], where $|\Xi\rangle$ runs over two-electron states, $:\cdots:$ normal-orders bilinear operators of bath electrons, $\mu\nu\neq 00$ and ls indices are contracted implicitly. The Kondo couplings are anti-ferromagnetic (>0) and of order $O(\Delta_0/U)$.

Several limits are well studied. $J_S=J_D=0$ enjoys a full SU(4) symmetry, and one channel of SU(4) bath is known to exactly screen the SU(4) impurity to form FL [54,92,93]. Increasing $J_S=J_D$ in either sign breaks SU(4) into commuting spin-SU(2) and valley-SU(2) groups. As $J_S=J_D<0$ becomes more negative, S and D gradually disappear from the low-energy space, leaving an effective SU(2) spin-1 two-channel Kondo model, which is also FL at low energy [92,94]. Physics at $J_S=J_D>0$ is equivalent to $J_S=J_D<0$ with the roles of "spin" and "valley" exchanged. Since removing or recovering either triplet does not interrupt the exact screening, the full diagonal line $J_S=J_D$ will be FL.

As valley-SU(2) is not guaranteed in real materials, $J_S\neq J_D$. Depending on which multiplet is the lowest, we divide the parameter space into three regimes. In the triplet regime ($J_{S,D}<0$), splitting occurs in the high-energy subspace, hence does not affect the low-energy FL phase. In the doublet ($0<J_D$, $J_S<J_D$) or singlet ($0<J_S$, $J_D<J_S$) regimes, however, splitting can eventually remove the Kondo resonance.

FL Phase

The FL phase manifests a coherent Kondo peak in the impurity spectral function $A_f(\omega)$ at $\omega=0$, which is adiabatically renormalized from the resonant peak in the non-interacting limit ($U=J_{S,D}=0$), and indicates the heavy quasiparticles are well-defined at energies lower than the Kondo temperature T_K. T_K is the inverse of quasiparticle lifetime due to hybridization with the bath. It decreases exponentially when increasing U/Δ_0, and defines a universal energy scale at low energy. By symmetry, the renormalized interactions between quasiparticles obey the same form as the bare ones, and we denote them as $\widetilde{U}$ and $\widetilde{J}_{S,D}$. Due to the continuous symmetry generated by $\sigma^0\varsigma^0$ (charge), $\sigma^0\varsigma^z$ (spin), and $\sigma^z\varsigma^0$ (valley), the corresponding quasiparticle susceptibilities $\chi_{c,s,v}$ [95–98] can be exactly obtained by the Ward identities [99–101] as [91]

$$\frac{\pi T_K}{4}\begin{pmatrix}\chi_c\\ \chi_s\\ \chi_v\end{pmatrix}=1-\frac{1}{\pi T_K}\begin{pmatrix}3 & -1 & -\frac{1}{2}\\ -1 & 1 & \frac{1}{2}\\ -1 & -1 & \frac{1}{2}\end{pmatrix}\begin{pmatrix}\widetilde{U}\\ \widetilde{J}_D\\ \widetilde{J}_S\end{pmatrix}. \tag{2}$$

Knowledge of $\chi_{c,s,v}$ allows us to constrain $\widetilde{U}$ and $\widetilde{J}_{S,D}$. Note that such renormalized interactions are related to the eigenvalues of the full local vertex function at zero frequency [91], and thus can be used to compute various lattice susceptibilities [102].

The strong U freezes the charge susceptibility at the Kondo energy scale, which implies $\chi_c\ll T_K^{-1}$. In the SU(4) symmetric limit where $\widetilde{J}_D=\widetilde{J}_S=0$, substituting $\chi_c\ll T_K^{-1}$ into Eq. (2) fixes $\widetilde{U}=\pi T_K/3$. Therefore, all channels are repulsive in this limit. When SU(4) is broken down to valley-SU(2), we first consider the limit of $J_D=J_S\gg T_K$. There, as the low-energy impurity states $S\oplus D$ do not carry spin, the local spin susceptibility also freezes. Substituting $\chi_{c,s}\ll T_K^{-1}$ and $\widetilde{J}_D=\widetilde{J}_S$ into Eq. (2) then solves that the $S\oplus D$ channel turns attractive, with effective FL interaction $\widetilde{U}-\widetilde{J}_{S,D}=-(\pi T_K/3)$. In the opposite limit of $J_D=J_S<0$ and $-J_{D,S}\gg T_K$, by exchanging "spin" and "valley", one can similarly conclude that the T channel turns attractive with $\widetilde{U}=-(\pi T_K/3)$ [98]. Between these limits, χ_s and hence the effective FL interaction parameters interpolate smoothly. In Fig. 1(b), we mark out the parameter regions where at least one FL interaction channel is attractive with the dashed lines.

Doublet Regime

To study the phase transition, consider the low-energy theory involving the bath and the D manifold $|L^z\rangle$, with Pauli matrices $\Lambda_z=|2\rangle\langle 2|-|\bar{2}\rangle\langle\bar{2}|$, and $\Lambda_+=\Lambda_-^\dagger=|2\rangle\langle\bar{2}|$. The only allowed Kondo coupling is $H_z\sim(2\pi\rho_z)\Lambda_z:\psi^\dagger\sigma^z\varsigma^0\psi:|_{x=0}$, which generates a phase shift of $2\pi\rho_z l\Lambda_z$ to bath electron flavor ls, in subspaces that diagonalize $\Lambda_z=\pm$ [92,103,104]. $\rho_z>0$ as the Kondo coupling is anti-ferromagnetic, and $\rho_z<1/2$ as the maximal phase shifts saturate to $\pm\pi$. Crucially, $\Lambda_\pm$ cannot appear in the Kondo coupling, as they alter the impurity valley-charge by ±4, which cannot be compensated by scattering one bath electron. However, two successive Kondo scatterings can link $|L^z\rangle$ to $|\overline{L^z}\rangle$ via a virtual excitation to S or T [Fig. 1(a)], scattering a pair of bath electrons to the opposite valley in total. We term

it as a pair-Kondo (PK) coupling, which by symmetries must read

$$H_x = (2\pi)^2 \lambda_x x_c \cdot \Lambda_+ \cdot \psi^\dagger_{-\uparrow}\psi^\dagger_{-\downarrow}\psi_{+\downarrow}\psi_{+\uparrow}\big|_{x=0} + \text{h.c.}, \tag{3}$$

where $\lambda_x \sim O((\Delta_0^2/U^2)(1/x_c J))$ is real, and x_c is a microscopic length scale. Hereafter we reserve J for the minimal multiplet excitation energy. In the doublet regime, $J = \min\{J_D, J_D - J_S\}$. The sign of λ_x is a gauge choice, as it can be reversed by a gauge transformation $\mathrm{i}\Lambda_z$. The total effective Hamiltonian sums to $H_{PK} = H_0 + H_z + H_x$.

We bosonize the chiral bath, $\psi_{ls}(x) \sim \mathrm{e}^{-\mathrm{i}\phi_{ls}(x)}/\sqrt{2\pi x_c}$ [103–111], where $\phi_{ls}(x)$ is a boson field that encodes the bath electron density in the ls flavor, $(1/2\pi)\partial_x\phi_{ls}(x) \sim :\psi^\dagger_{ls}(x)\psi_{ls}(x):$, and obeys $[\phi_{ls}(x), \phi_{l's'}(x')] = -\mathrm{i}\pi\delta_{ls,l's'}\mathrm{sgn}(x-x')$. For our purpose here, we have kept the Klein factors implicit and ignored the finite-size terms by taking the thermodynamic limit. A rigorous mapping between the fermion and boson representations that includes these terms is presented in Ref. [90]. In H_{PK}, only one combination of boson fields, $\phi_v = \sum_{ls}(l/2)\phi_{ls}$, couples to the impurity, which corresponds to the fluctuation of valley charge density. The other three combinations orthogonal to ϕ_v decouple, which encode the density fluctuations of electric charge (ϕ_c), spin (ϕ_s), and valley-contrasting spin (ϕ_{vs}), respectively.

The phase shifts induced by H_z can be absorbed by a unitary transformation $\mathcal{U} = \mathrm{e}^{\mathrm{i}2\rho_z\Lambda_z\phi_v(0)}$, as $\mathcal{U}\psi_{ls}(x)\mathcal{U}^\dagger = \psi_{ls}(x)\mathrm{e}^{\mathrm{i}\pi\rho_z l\Lambda_z \mathrm{sgn}(x)}$. Therefore, $\overline{H}_{PK} = \mathcal{U}H_{PK}\mathcal{U}^\dagger = H_0 + \overline{H}_x$, where H_0 still denotes the (bosonized) free bath Hamiltonian. Since $\mathcal{U}\Lambda_\pm\mathcal{U}^\dagger = \Lambda_\pm \mathrm{e}^{\pm\mathrm{i}4\rho_z\phi_v(0)}$, the PK term is dressed as

$$\overline{H}_x = \mathcal{U}H_x\mathcal{U}^\dagger = \frac{\lambda_x}{x_c}\cdot\Lambda_+ \cdot \mathrm{e}^{-\mathrm{i}\gamma\phi_v(0)} + \text{h.c.}, \tag{4}$$

with $\gamma = 2 - 4\rho_z$. Vertex operators $\mathrm{e}^{\mathrm{i}\gamma\phi_v(x)}$ obey $\langle \mathrm{e}^{\mathrm{i}\gamma\phi_v(x,\tau)}\mathrm{e}^{-\mathrm{i}\gamma\phi_v(x,\tau')}\rangle_0 \sim |\tau-\tau'|^{-\gamma^2}$ under time-evolution of H_0, where $\phi_v(x,\tau) = \mathrm{e}^{\tau H_0}\phi_v(x)\mathrm{e}^{-\tau H_0}$ and $\langle\cdots\rangle_0$ averages over the zero-temperature ensemble of H_0, which implies their scaling dimension $[\mathrm{e}^{\mathrm{i}\gamma\phi_v}] = \gamma^2/2$. Given that $[\overline{H}_x] = 1$ scales with the energy dimension, there must be $[\lambda_x] = 1 - (\gamma^2/2)$, suggesting an RG flow under $\tau \to \tau\mathrm{e}^{\mathrm{d}\ell}$

$$\frac{\mathrm{d}\lambda_x}{\mathrm{d}\ell} = \left(1 - \frac{\gamma^2}{2}\right)\lambda_x = (-1 + 8\rho_z - 8\rho_z^2)\lambda_x. \tag{5}$$

$\rho_z^c = (1/2) - (1/2\sqrt{2}) \approx 0.1464$ is the critical value, above which λ_x turns relevant.

To derive the RG flow of γ (hence ρ_z), we express the total partition function Z perturbatively in λ_x,

$$\frac{Z}{Z_0} = \left\langle T_\tau \mathrm{e}^{-\int_0^\infty \mathrm{d}\tau \overline{H}_x(\tau)}\right\rangle_0 = \sum_{n=0}^{\infty}\delta Z_{2n},$$

where Z_0 is the free partition function of H_0, $\overline{H}_x(\tau) = \mathrm{e}^{\tau H_0}\overline{H}_x\mathrm{e}^{-\tau H_0}$, and δZ_{2n} collects the $O(\lambda_x^{2n})$ order terms. Odd order terms vanish as H_0 conserves Λ_z. δZ_{2n} sums over trajectories along the τ axis that flip the impurity by $2n$ times: if starting from the $\Lambda_z = -$ sector, there are $\Lambda_+\mathrm{e}^{-\mathrm{i}\gamma\phi_v}$ at τ_{2k-1} and $\Lambda_-\mathrm{e}^{\mathrm{i}\gamma\phi_v}$ at τ_{2k} ($\tau_1 < \cdots < \tau_{2n}$); and the $\Lambda_z = +$ sector follows similarly.

Each flipping occurs with probability λ_x, and each pair of flippings at $\tau_i < \tau_j$ contributes a factor of $|\tau_i - \tau_j|^{(-1)^{i-j}\gamma^2} = \mathrm{e}^{(-1)^{i-j}\gamma^2 \ln|\tau_i-\tau_j|}$ [90], due to the correlation between dressed vertex operators. The latter exponent can then be interpreted as a "two-dimensional Coulomb potential" between $2n$ classical particles [112,113]: the particle at τ_i carries "charge" $(-1)^i$ and is created with fugacity λ_x. The corresponding Coulomb strength is proportional to γ^2. Upon coarse-graining, two adjacent particles within a short distance will form a virtual dipole, oriented to screen the Coulomb potential between the remaining particles, implying $\mathrm{d}(\gamma^2)/\mathrm{d}\ell \propto -\lambda_x^2\gamma^2$, namely $\mathrm{d}\rho_z/\mathrm{d}\ell \propto (1-2\rho_z)\lambda_x^2$. Detailed calculations fix the proportionality [90],

$$\frac{\mathrm{d}\rho_z}{\mathrm{d}\ell} = (1-2\rho_z)\lambda_x^2. \tag{6}$$

As $\rho_z \in (0, 1/2)$, ρ_z always grows. Eqs. (5) and (6) are exact in ρ_z albeit approximate to $O(\lambda_x^3)$ order, taking the standard Berezinskii–Kosterlitz–Thouless (BKT) form Ref. [110], with the flow diagram drawn in Fig. 1(c). Our NRG calculations also verify this BKT transition in the full Anderson model [91]. We term the continuous fixed line along $\lambda_x = 0$, $\rho_z < \rho_z^c$ as the anisotropic doublet (AD) phase, where the system flows to a non-universal ρ_z depending on initial parameters. Beyond ρ_z^c, λ_x grows into a strong-coupling regime, which we next demonstrate as a FL phase of PK resonance.

FL in Doublet Regime

At $\rho_z^\star = 1/4 > \rho_z^c$, the vertex operator appearing in $\overline{H}_x$ [Eq.(4)] reads $\mathrm{e}^{-\mathrm{i}\phi_v(x)}$, allowing for a refermionization $\psi_v(x) \sim \mathrm{e}^{-\mathrm{i}\phi_v(x)}/\sqrt{2\pi x_c}$ [103,105–109]. ψ_v only alters the bath valley charge, and encodes the corresponding valley density fluctuation, while commutes with other quantum numbers and density channels. Meanwhile, Λ_- can also be mapped into a fermion operator f_v, which can be constructed as anticommuting with $\psi_v(x)$ after attaching a Jordan-Wigner string that counts the bath valley charges [90]. Therefore, $\overline{H}_x = \sqrt{2\pi/x_c}\lambda_x f_v^\dagger\psi_v(0) +$ h.c. is mapped to a fermionic bilinear term and exactly solvable, which describes a resonant level f_v embedded in the bath of ψ_v, with linewidth $T_K = \pi\lambda_x^2/x_c$. At temperature below T_K, f_v cannot stay empty nor fully occupied, but must hybridize into the bath, implying that the local entropy freezes to 0. The impurity is thus fully screened into a FL due to the PK process. In Ref. [90], we further solve the finite-size many-body spectrum, and show the low-energy end differs from the free bath spectrum only by a π phase-shift. We also show the susceptibilities of $\Lambda_{\pm,z}$ to obey the typical FL scaling, $\mathrm{Im}\chi_{\pm,z}(\omega + \mathrm{i}0^+) \sim \omega$ at $\omega \ll T_K$. These results all confirm the FL behavior.

Since bringing down S, T states into the low-energy space does not interrupt the exact screening, FL in the doublet regime can cross over to FL in other regimes. Nonetheless, the renormalized interaction behaves differently. A special limit is $J_S = 0$, where the global spin-SU(2) is enhanced into two independent SU(2) rotations in $l = \pm$ valleys, generated by $((\sigma^0 \pm \sigma^z)/2)\varsigma^{x,y,z}$. Such symmetry locks S and T as degenerate, hence $\widetilde{J}_S = 0$. When $T_K \ll J_D$, $\chi_c, \chi_s \ll T_K^{-1}$, and solving Eq. (2) shows that D is the only attractive channel, with $\widetilde{U} - \widetilde{J}_D = -\pi T_K$ [114]. As splitting $J_S \neq 0$ in the high-energy end should not affect low-energy physics, the D channel will remain attractive as long as $T_K \ll J$.

Anisotropic Doublet

At the fixed line ($\lambda_x = 0$, $\rho_z < \rho_z^c$), Λ_z is conserved and hence unscreened. Its static susceptibility thus obeys the Curie's law, $\chi_v \sim T^{-1}$. On the other hand, the impurity flipping is dressed into $\mathcal{U}\Lambda_\pm\mathcal{U}^\dagger = \Lambda_\pm\mathrm{e}^{\pm\mathrm{i}4\rho_z\phi_v(0)}$, implying its correlation function $\chi_\pm(\tau) \sim |\tau|^{-(4\rho_z)^2}$. Therefore, the corresponding dynamic susceptibility scales in a non-universal power law, $\mathrm{Im}\chi_\pm(\omega + \mathrm{i}0^+) \sim \mathrm{sgn}(\omega)|\omega|^{16\rho_z^2-1}$, and the static susceptibility diverges as $\chi_\pm \sim T^{16\rho_z^2-1}$.

The impurity spectral function $A_f(\omega)$ is proportional to the scattering $\mathcal{T}$-matrix of bath electrons [115–117], and the latter remains well-defined in the downfolded model H_{PK}. According to the equation of motion $[H_z + H_x, \psi_{+\uparrow}(0)]$, $\psi_{+\uparrow}(0)$ scatters into two pieces: $\widetilde{f}^{(1)}_{+\uparrow} \sim \rho_z\Lambda_z\psi_{+\uparrow}\big|_{x=0}$ and $\widetilde{f}^{(2)}_{+\uparrow} \sim (2\pi\lambda_x x_c)\Lambda_-\psi^\dagger_{+\downarrow}\psi_{-\downarrow}\psi_{-\uparrow}\big|_{x=0}$, where ρ_z, λ_x are the un-renormalized parameters in H_{PK}. The $\mathcal{T}$-matrix is then given by the Green's function of $\widetilde{f}^{(1)}_{+\uparrow} + \widetilde{f}^{(2)}_{+\uparrow}$, whose long-time behavior is governed by the AD fixed point Hamiltonian. As Λ_z is conserved there, $\widetilde{f}^{(1,2)}_{+\uparrow}$ do not mix. The time-evolution of $\widetilde{f}^{(1)}_{+\uparrow}$ is solely governed by $\psi_{+\uparrow}$, which produces a spectrum proportional to the bath density of states, $A_f^{(1)}(\omega) \sim \text{const}$. On the other hand, as

$$\mathcal{U}\widetilde{f}^{(2)}_{+\uparrow}\mathcal{U}^\dagger \sim \Lambda_-\mathrm{e}^{-\frac{\mathrm{i}}{2}(\phi_c+\phi_s+\phi_{vs})}\mathrm{e}^{\mathrm{i}\left(\frac{3}{2}-4\rho_z\right)\phi_v}\big|_{x=0},$$

the Green's function of $\widetilde{f}^{(2)}_{+\uparrow}$ scales as $|\tau|^{-\alpha_2}$, where $\alpha_2 = 3/4 + (3/2 - 4\rho_z)^2$ sums over the scaling exponent of all four boson channels, implying a spectral function $A_f^{(2)}(\omega) \sim |\omega|^{\alpha_2 - 1}$. $0 < \rho_z < \rho_z^c$ maps to $2 > \alpha_2 - 1 > 2 - \sqrt{2} \approx 0.5858$ monotonically, hence near the BKT transition ρ_z^c, $A_f^{(2)}(\omega)$ behaves as a non-analytic kink depicted in Fig. 2(a), which contrasts significantly to the Kondo peak in FL.

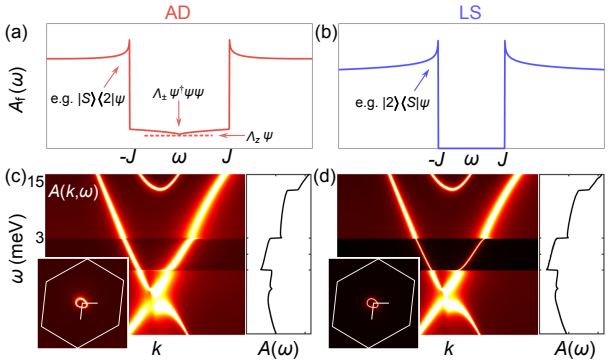

Fig. 2. (a) and (b) $A_f(\omega)$ obtained from bosonization. Pseudogap shoulders ($A_f^{(3)}$) are multiplet excitations, induced by scattering a bath electron ($\omega \leqslant -J$) or hole ($\omega \geqslant J$). They are symmetrically pinned around the Fermi energy. For the AD phase, residual longitudinal coupling contributes a constant background ($A_f^{(1)}$, dashed line), while the irrelevant PK coupling contributes a non-analytic kink ($A_f^{(2)}$) above it. (c) and (d) Lattice spectral function $A(k,\omega)$ in one valley, obtained using the *ansätze* of $\Sigma_f(\omega)$ derived from single impurity. Insets are contours at $\omega = 0$, with hexagons denoting the strained moiré Brillouin zone, and white lines indicating the k-path of main figures. AD does not have a well-defined Fermi surface, while LS is a Fermi liquid of c electrons only. $A(\omega) = \int (\mathrm{d}^2k/(2\pi)^2) A(k,\omega)$ is proportional to the total density of states.

Pseudogap

Following the same reasoning, we investigate $A_f(\omega)$ at $\omega \sim O(J)$, where the effective theory is the Kondo Hamiltonian. For simplicity, let us assume $0 < J_S < J_D$, and first include S into the low-energy space, so that the Kondo Hamiltonian reads $H_K = H_0 + H_J + H_z + H_{x0}$. $H_J = J|S\rangle\langle S|$ denotes the multiplet excitation with $J = J_D - J_S$, and the Kondo coupling between S and D reads $H_{x0} = (2\pi\zeta_x)\Theta_+ : \psi^\dagger\sigma^-\varsigma^0\psi : +\mathrm{h.c.}$, where $\sigma^\pm = (\sigma^x \pm \mathrm{i}\sigma^y)/2$, and $\Theta_+ = \Theta_-^\dagger = |S\rangle\langle\bar{2}| + |2\rangle\langle S|$. Therefore, $\psi_{+\uparrow}(0)$ also scatters into $\widetilde{f}^{(3)}_{+\uparrow} = (2\pi\zeta_x)\Theta_-\psi_{-\uparrow}$, whose motion will contribute an $A_f^{(3)}(\omega)$. The phase shift dresses $\widetilde{f}^{(3)}_{+\uparrow}$ into

$$\mathcal{U}\widetilde{f}^{(3)}_{+\uparrow}\mathcal{U}^\dagger \sim \Theta_- \cdot \mathrm{e}^{-\frac{\mathrm{i}}{2}(\phi_c+\phi_s-\phi_{vs})}\mathrm{e}^{\mathrm{i}\left(\frac{1}{2}-2\rho_z\right)\phi_v}\Big|_{x=0}.$$

Since Θ_- excites D to S, the minimal energy cost is J, leading to a threshold factor $\theta(|\omega|-J)$ in $A_f^{(3)}(\omega)$. Meanwhile, the accompanying bath vertex operators of all four boson channels contribute a total correlation as $|\tau|^{-\alpha_3}$, with $\alpha_3 = 3/4 + (1/2 - 2\rho_z)^2 < 1$. Combining the two parts, we find $A_f^{(3)}(\omega) \sim \theta(|\omega|-J)\big||\omega|-J\big|^{\alpha_3-1}$ [91], forming the pseudogap shoulder [Fig. 2(a)]. Since terms irrelevant at the AD fixed point can be important at such a high energy scale, quantitative behaviors around the shoulders can be altered, e.g., the sharp step function $\theta(|\omega|-J)$ could be broadened. Further including T will bring in another set of shoulders at $\omega = \pm J_D$.

Singlet Regime

Unlike the doublet regime, if the low-energy space is restricted to S, the impurity will have no internal degrees of freedom, hence decouple from the bath. We term this phase as the local singlet (LS) phase. To understand the phase transition, we put back D, assuming $J_S > J_D > 0$, and now denoting $J = J_S - J_D > 0$. The effective Kondo Hamiltonian H_K takes a similar form as in the last paragraph, except that we replace $H_J = J\Lambda_z^2$ in this regime. Since J has the energy dimension ($[J] = 1$), it grows under RG without ζ_x. For any $\rho_z > 0$, the Kondo coupling ζ_x will also have a relevant scaling dimension, as in the spin-1 two-channel Kondo problem. However, since a large ζ_x tends to overcome the excitation cost of J, while a large J suppresses the scattering amplitude of ζ_x, they generate quantum corrections that reduce each other (detailed calculations are presented in Ref. [90]). By this competition, FL ($\zeta_x \to \infty, J \to 0$) and LS ($J \to \infty, \zeta_x \to 0$) are separated by an unstable fixed point as shown by Fig. 1(d). This phase transition is consistent with previous NRG studies in similar models [114,118,119], where the critical point is found to be described by a non-Fermi liquid with impurity entropy $\ln\sqrt{2}$ [118]. If $J_S > 0 > J_D$, on the other hand, the low-energy space consists of $S \oplus T$, and the phase transition should be equivalent to that in the two-impurity Kondo problem [120–127], which was also found to be second-order.

As the S state carries no symmetry charge, $\chi_{c,s,v} \ll T_K^{-1}$ all freeze in FL if $T_K \ll J$. Solving Eq. (2) finds the S channel is the only attractive one, with $\widetilde{U} - \widetilde{J}_S = -3\pi T_K$ [119].

The fixed-point Hamiltonian of LS only contains H_0, hence bath electrons do not scatter and $A_f(\omega) \to 0$ as $\omega \to 0$, in contrast to the in-gap excitations of AD. As $A_f(\omega) = -(1/\pi)\,\mathrm{Im}\,1/(\omega + \mathrm{i}\Delta_0 - \Sigma_f(\omega))$, where the hybridization Δ_0 is finite, this indicates a pole in $\Sigma_f(\omega) \sim 1/\omega$. Particle-hole asymmetry can lead to a scattering potential of: $\psi^\dagger\sigma^0\varsigma^0\psi :|_{x=0}$ hence a small finite $A_f(0)$, but does not affect the pole structure [91]. The pseudogap shoulders, however, form by the same mechanism as in AD, and represent multiplet excitations to the D or T states induced by scattering a bath electron or hole [Fig. 2(b)].

Correlation Self-Energy

The single-impurity solutions [Fig. 1(b)] shed light into the lattice problem of periodic spin-valley Anderson impurities. In separate papers [87], we show that the quantum phase transitions into the AD and LS phases obtained via local analysis can indeed appear in the normal-state DMFT solution of MATBG [48] around filling fractions $\nu \approx \pm 2$, if the corresponding anti-Hund's rule is present. We remind, however, that the lattice counterpart of AD phase cannot persist to zero temperature due to the large entropy contributed by the local degeneracies, and spontaneous symmetry-breaking can happen for both AD and LS phases on the lattice around the transition points, and replace the transitions between normal states. For a sketchy understanding to the lattice spectral function $A(k,\omega)$ of the AD and LS phases across the full frequency span, we construct analytical *anšatz* for the correlation self-energy $\Sigma_f(\omega)$ that qualitatively reproduces the single-impurity $A_f(\omega)$, including Hubbard peaks, pseudogap shoulders, and in-gap features [91], which we then insert into the lattice Green's function. Local FL leads to a heavy Fermi liquid on the lattice, with a Fermi volume $\nu/4$, where both f and c electrons contribute [53–60]. If higher multiplets that do not participate in Kondo resonance exist, pseudogap shoulders similar to Figs. 2(a) and 2(b) can also be found, besides the Kondo resonance peak around $\omega = 0$. Increasing J_S locks each impurity into a LS, and $\Sigma_f \sim 1/\omega$ at $\omega \ll J$ gaps out the heavy f quasiparticles. Correspondingly, the Fermi volume jumps to $(\nu - 2\mathrm{sgn}(\nu))/4$ [Fig. 2(d)] [128], where $\nu_f \approx \pm 2$ disappears. At $\nu = 2$, the lattice forms a symmetric Mott phase [84,87,129]. Contrarily, on increasing J_D into the AD phase, an unscreened doublet per unit cell remains. At finite temperature where no further spontaneous symmetry breaking occurs, the in-gap excitations of A_f pervade the Brillouin zone. Moving in a highly disordered landscape with randomly oriented doublets, c-electrons also acquire a finite lifetime [Fig. 2(c)].

Discussion

In the AD and LS phases, despite that the f heavy quasiparticle has vanished, the local pairing susceptibilities in the D and S channel, respectively, are still well-defined, and found enhanced [87]. In the AD phase, the enhancement can be understood as a residual effect from λ_x [Eq. (3)] at the intermediate energy scales, which allows the charge-two excitations forming the D representation to lower energy by coupling to $\Lambda_\pm$ [91], compared to two independent charge-one excitations. Deep in the LS phase, the enhancement can be understood as an effective interaction among c-electrons at $x = 0$, induced by virtual impurity multiplet fluctuations [91]. Approaching the critical point between LS and FL, the enhancement is closely related to a relevant operator that violates charge-U(1) at the critical point [118].

On lowering temperature, superconductivity may develop from different normal states, due to the local pairing potentials summarized

in Fig. 1(b), forming a lower superconductivity tunneling gap. On the other hand, as the pseudogap shoulders form at a higher energy scale (Fig. 2) set by the anti-Hund's J, they should also persist in the superconducting phase. This provides a potential explanation to the two-gap structure found by Refs. [38,39]. Simultaneously, in the anti-Hund's regime ($J_{S,D} > 0$), the valley moments spanned by $S \oplus D$ also couple to one another via Ruderman–Kittel–Kasuya–Yosida (RKKY) interactions. When the RKKY interaction is strong, the valley moments can align, leading to spontaneous symmetry breaking into either valley-polarized or inter-valley-coherent (IVC) [21,22] states, which can coexist with superconductivity. To clarify the interplay between superconductivity and IVC orders will be a crucial next step toward a complete theory of MATBG/TTG.

Note Added

After posting this work, we became aware of a related study [130] that shares a similar perspective on the origin of pairing and pseudogap in MATBG.

Acknowledgments

We thank Hyunjin Kim and Jeong Min Park for fruitful discussions. Z.-D. S., Y.-J. W., and G.-D. Z. were supported by the National Natural Science Foundation of China (Grant No. 12274005), the National Key Research and Development Program of China (Grant No. 2021YFA1401900), and the Quantum Science and Technology-National Science and Technology Major Project (Grant No. 2021ZD0302403). H. J., S. Y., and S.-S. B. L. were supported by the National Research Foundation of Korea (NRF) funded by the Korean government (MSIT: Grant Nos. RS-2023-00214464, RS-2023-00258359, RS-2023-NR119931, and RS-2024-00442710; MEST: Grant No. 2019R1A6A1A10073437), the Global-LAMP Program funded by the Ministry of Education (Grant No. RS-2023-00301976), and Samsung Electronics Co., Ltd. (Grant No. IO220817-02066-01).

References

[1] Andrei E Y and MacDonald A H 2020 *Nat. Mater.* **19** 1265
[2] Mak K F and Shan J 2022 *Nat. Nanotechnol.* **17** 686
[3] Nuckolls K P and Yazdani A 2024 *Nat. Rev. Mater.* **9** 460
[4] Wu F, Lovorn T, Tutuc E, and MacDonald A H 2018 *Phys. Rev. Lett.* **121** 026402
[5] Koshino M, Yuan N F Q, Koretsune T, Ochi M, Kuroki K, and Fu L 2018 *Phys. Rev. X* **8** 031087
[6] Haule M, Andrei E Y, and Haule K 2019 arXiv: 1901.09852 [cond-mat.str-el]
[7] Liu J, Liu J, and Dai X 2019 *Phys. Rev. B* **99** 155415
[8] Calderón M J and Bascones E 2020 *Phys. Rev. B* **102** 155149
[9] Reddy A P, Devakul T, and Fu L 2023 *Phys. Rev. Lett.* **131** 246501
[10] Liu Y, Aryal A, Calugaru D, Fang Z, Yang K, Hu H, Yan Q, Bernevig B A, and Liu C X 2025 arXiv: 2507.06168 [cond-mat.mes-hall]
[11] Chen C, Nuckolls K P, Ding S, Miao W, Wong D, Oh M, Lee R L, He S, Peng C, Pei D, Li Y, Hao C, Yan H, Xiao H, Gao H, Li Q, Zhang S, Liu J, He L, Watanabe K, Taniguchi T, Jozwiak C, Bostwick A, Rotenberg E, Li C, Han X, Pan D, Liu Z, Dai X, Liu C, Bernevig B A, Wang Y, Yazdani A, and Chen Y 2024 *Nature* **636** 342
[12] Birkbeck J, Xiao J, Inbar A, Taniguchi T, Watanabe K, Berg E, Glazman L, Guinea F, von Oppen F, and Ilani S 2025 *Nature* **641** 345
[13] Bistritzer R and MacDonald A H 2011 *Proc. Natl. Acad. Sci. U.S.A.* **108** 12233
[14] Cao Y, Fatemi V, Demir A, Fang S, Tomarken S L, Luo J Y, Sanchez-Yamagishi J D, Watanabe K, Taniguchi T, Kaxiras E, Ashoori R C, and Jarillo-Herrero P 2018 *Nature* **556** 80
[15] Lu X, Stepanov P, Yang W, Xie M, Aamir M A, Das I, Urgell C, Watanabe K, Taniguchi T, Zhang G, Bachtold A, MacDonald A H, and Efetov D K 2019 *Nature* **574** 653
[16] Choi Y, Kemmer J, Peng Y, Thomson A, Arora H, Polski R, Zhang Y, Ren H, Alicea J, Refael G, von Oppen F, Watanabe K, Taniguchi T, and Nadj-Perge S 2019 *Nat. Phys.* **15** 1174
[17] Kerelsky A, McGilly L J, Kennes D M, Xian L, Yankowitz M, Chen S, Watanabe K, Taniguchi T, Hone J, Dean C, Rubio A, and Pasupathy A N 2019 *Nature* **572** 95
[18] Jiang Y, Lai X, Watanabe K, Taniguchi T, Haule K, Mao J, and Andrei E Y 2019 *Nature* **573** 91
[19] Xie Y, Lian B, Jäck B, Liu X, Chiu C L, Watanabe K, Taniguchi T, Bernevig B A, and Yazdani A 2019 *Nature* **572** 101
[20] Nuckolls K P, Oh M, Wong D, Lian B, Watanabe K, Taniguchi T, Bernevig B A, and Yazdani A 2020 *Nature* **588** 610
[21] Nuckolls K P, Lee R L, Oh M, Wong D, Soejima T, Hong J P, Călugăru D, Herzog-Arbeitman J, Bernevig B A, Watanabe K, Taniguchi T, Regnault N, Zaletel M P, and Yazdani A 2023 *Nature* **620** 525
[22] Kim H, Choi Y, Lantagne-Hurtubise E, Lewandowski C, Thomson A, Kong L, Zhou H, Baum E, Zhang Y, Holleis L, Watanabe K, Taniguchi T, Young A F, Alicea J, and NadjPerge S 2023 *Nature* **623** 942
[23] Yankowitz M, Chen S, Polshyn H, Zhang Y, Watanabe K, Taniguchi T, Graf D, Young A F, and Dean C R 2019 *Science* **363** 1059
[24] Arora H S, Polski R, Zhang Y, Thomson A, Choi Y, Kim H, Lin Z, Wilson I Z, Xu X, Chu J H, Watanabe K, Taniguchi T, Alicea J, and Nadj-Perge S 2020 *Nature* **583** 379
[25] Saito Y, Ge J, Watanabe K, Taniguchi T, and Young A F 2020 *Nat. Phys.* **16** 926
[26] Stepanov P, Das I, Lu X, Fahimniya A, Watanabe K, Taniguchi T, Koppens F H L, Lischner J, Levitov L, and Efetov D K 2020 *Nature* **583** 375
[27] Liu X, Wang Z, Watanabe K, Taniguchi T, Vafek O, and Li J I A 2021 *Science* **371** 1261
[28] Cao Y, Rodan-Legrain D, Park J M, Yuan N F Q, Watanabe K, Taniguchi T, Fernandes R M, Fu L, and Jarillo-Herrero P 2021 *Science* **372** 264
[29] Cao Y, Park J M, Watanabe K, Taniguchi T, and Jarillo-Herrero P 2021 *Nature* **595** 526
[30] Park J M, Cao Y, Watanabe K, Taniguchi T, and Jarillo-Herrero P 2021 *Nature* **590** 249
[31] Hao Z, Zimmerman A M, Ledwith P, Khalaf E, Najafabadi D H, Watanabe K, Taniguchi T, Vishwanath A, and Kim P 2021 *Science* **371** 1133
[32] Kim H, Choi Y, Lewandowski C, Thomson A, Zhang Y, Polski R, Watanabe K, Taniguchi T, Alicea J, and Nadj-Perge S 2022 *Nature* **606** 494
[33] Liu X, Zhang N J, Watanabe K, Taniguchi T, and Li J I A 2022 *Nat. Phys.* **18** 522
[34] Gao X, Jimeno-Pozo A, Pantaleon P A, Codecido E, Sharifi D L, Zhang Z, Liu Y, Watanabe K, Taniguchi T, Bockrath M W, Guinea F, and Lau C N 2024 arXiv: 2412.01578 [cond-mat.mes-hall]
[35] Tanaka M, Wang J îj, Dinh T H, Rodan-Legrain D, Zaman S, Hays M, Almanakly A, Kannan B, Kim D K, Niedzielski B M, Serniak K, Schwartz M E, Watanabe K, Taniguchi T, Orlando T P, Gustavsson S, Grover J A, Jarillo-Herrero P, and Oliver W D 2025 *Nature* **638** 99
[36] Banerjee A, Hao Z, Kreidel M, Ledwith P, Phinney I, Park J M, Zimmerman A, Wesson M E, Watanabe K, Taniguchi T, Westervelt R M, Yacoby A, Jarillo-Herrero P, Volkov P A, Vishwanath A, Fong K C, and Kim P 2025 *Nature* **638** 93
[37] Oh M, Nuckolls K P, Wong D, Lee R L, Liu X, Watanabe K, Taniguchi T, and Yazdani A 2021 *Nature* **600** 240
[38] Park J M, Sun S, Watanabe K, Taniguchi T, and Jarillo-Herrero P 2026 *Science* **391** 79
[39] Kim H, Rai G, Crippa L, Călugăru D, Hu H, Choi Y, Kong L, Baum E, Zhang Y, Holleis L, Watanabe K, Taniguchi T, Young A F, Bernevig B A, Valentí R, Sangiovanni G, Wehling T, and Nadj-Perge S 2026 *Nature* **650** 592
[40] Polshyn H, Yankowitz M, Chen S, Zhang Y, Watanabe K, Taniguchi T, Dean C R, and Young A F 2019 *Nat. Phys.* **15** 1011
[41] Cao Y, Chowdhury D, Rodan-Legrain D, Rubies-Bigorda O, Watanabe K, Taniguchi T, Senthil T, and Jarillo-Herrero P 2020 *Phys. Rev. Lett.* **124** 076801
[42] Jaoui A, Das I, Di Battista G, Díez-Mérida J, Lu X, Watanabe K, Taniguchi T, Ishizuka H, Levitov L, and Efetov D K 2022 *Nat. Phys.* **18** 633
[43] Zou L, Po H C, Vishwanath A, and Senthil T 2018 *Phys. Rev. B* **98** 085435

[44] Song Z, Wang Z, Sh iW, Li G, Fang C, and Bernevig B A 2019 *Phys. Rev. Lett.* **123** 036401
[45] Po H C, Zou L, Senthil T, and Vishwanath A 2019 *Phys. Rev. B* **99** 195455
[46] Ahn J, Park S, and Yang B J 2019 *Phys. Rev. X* **9** 021013
[47] Wang J, Zheng Y, Millis A J, and Cano J 2021 *Phys. Rev. Res.* **3** 023155
[48] Song Z D and Bernevig B A 2022 *Phys. Rev. Lett.* **129** 047601
[49] Shi H and Dai X 2022 *Phys. Rev. B* **106** 245129
[50] Yu J, Xie M, Bernevig B A, and Das Sarma S 2023 *Phys. Rev. B* **108** 035129
[51] Singh K, Chew A, Herzog-Arbeitman J, Bernevig B A, and Vafek O 2024 *Nat. Commun.* **15** 5257
[52] Herzog-Arbeitman J, Yu J, Călugăru D, Hu H, Regnault N, Vafek O, Kang J, and Bernevig B A 2025 *Phys. Rev. B* **112** 125128
[53] Chou Y Z and Das Sarma S 2023 *Phys. Rev. Lett.* **131** 026501
[54] Zhou G D, Wang Y J, Tong N, and Song Z D 2024 *Phys. Rev. B* **109** 045419
[55] Rai G, Crippa L, Călugăru D, Hu H, Paoletti F, de' Medici L, Georges A, Bernevig B A, Valentí R, Sangiovanni G, and Wehling T 2024 *Phys. Rev. X* **14** 031045
[56] Hu H, Bernevig B A, and Tsvelik A M 2023 *Phys. Rev. Lett.* **131** 026502
[57] Hu H, Rai G, Crippa L, Herzog-Arbeitman J, Călugăru D, Wehling T, Sangiovanni G, Valentí R, Tsvelik A M, and Bernevig B A 2023 *Phys. Rev. Lett.* **131** 166501
[58] Chou Y Z and Das Sarma S 2023 *Phys. Rev. B* **108** 125106
[59] Datta A, Calderón M J, Camjayi A, and Bascones E 2023 *Nat. Commun.* **14** 5036
[60] Lau L L and Coleman P 2025 *Phys. Rev. X* **15** 021028
[61] Călugăru D, Hu H, Merino R L, Regnault N, Efetov D K, and Bernevig B A 2024 arXiv: 2402.14057 [cond-mat.str-el]
[62] Herzog-Arbeitman J, Călugăru D, Hu H, Yu J, Regnault N, Kang J, Bernevig B A, and Vafek O 2025 *Phys. Rev. B* **112** 125129
[63] Crippa L, Rai G, Călugăru D, Hu H, Herzog-Arbeitman J, Bernevig B A, Valentí R, Sangiovanni G, andWehling T 2025 arXiv: 2509.19436 [cond-mat.str-el]
[64] Călugăru D, Hu H, Crippa L, Rai G, Regnault N, Wehling T O, Valentí R, Sangiovanni G, and Bernevig B A 2025 arXiv: 2509.18256 [cond-mat.str-el]
[65] Rozen A, Park J M, Zondiner U, Cao Y, Rodan-Legrain D, Taniguchi T, Watanabe K, Oreg Y, Stern A, Berg E, Jarillo-Herrero P, and Ilani S 2021 *Nature* **592** 214
[66] Saito Y, Yang F, Ge J, Liu X, Taniguchi T, Watanabe K, Li J I A, Berg E, and Young A F 2021 *Nature* **592** 220
[67] Zhang Z, Wu S, Călugăru D, Hu H, Taniguchi T, Wanatabe K, Bernevig A B, and Andrei E Y 2025 arXiv: 2503.17875 [cond-mat.mes-hall]
[68] Zondiner U, Rozen A, Rodan-Legrain D, Cao Y, Queiroz R, Taniguchi T, Watanabe K, Oreg Y, von Oppen F, Stern A, Berg E, Jarillo-Herrero P, and Ilani S 2020 *Nature* **582** 203
[69] Wong D, Nuckolls K P, Oh M, Lian B, Xie Y, Jeon S, Watanabe K, Taniguchi T, Bernevig B A, and Yazdani A 2020 *Nature* **582** 198
[70] Hu Q, Liang S, Li X, Shi H, Dai X, and Xu Y 2024 arXiv: 2406.08734 [cond-mat.mes-hall]
[71] Merino R L, Călugăru D, Hu H, Díez-Mérida J, Díez-Carlón A, Taniguchi T, Watanabe K, Seifert P, Bernevig B A, and Efetov D K 2025 *Nat. Phys.* **21** 1078
[72] Xiao J, Inbar A, Birkbeck J, Gershon N, Zamir Y, Taniguchi T, Watanabe K, Berg E, and Ilani S 2025 arXiv: 2506.20738 [cond-mat.mes-hall]
[73] Wu F, MacDonald A H, and Martin I 2018 *Phys. Rev. Lett.* **121** 257001
[74] Lian B, Wang Z, and Bernevig B A 2019 *Phys. Rev. Lett.* **122** 257002
[75] Koshino M and Nam N N T 2020 *Phys. Rev. B* **101** 195425
[76] Cea T and Guinea F 2021 *Proc. Natl. Acad. Sci. U.S.A.* **118** e2107874118
[77] Liu X, Peng R, Sun Z, and Liu J 2022 *Nano Lett.* **22** 7791
[78] Liu C X, Chen Y, Yazdani A, and Bernevig B A 2024 *Phys. Rev. B* **110** 045133
[79] Zhu Z and Devereaux T P 2025 arXiv: 2407.03293 [cond-mat.mes-hall]
[80] Lau L L H, Gleis A, Kaplan D, Chandra P, and Coleman P 2025 *Phys. Rev. B* **111** 245149
[81] Dodaro J F, Kivelson S A, Schattner Y, Sun X Q, and Wang C 2018 *Phys. Rev. B* **98** 075154
[82] Angeli M, Tosatti E, and Fabrizio M 2019 *Phys. Rev. X* **9** 041010
[83] Blason A and Fabrizio M 2022 *Phys. Rev. B* **106** 235112
[84] Wang Y J, Zhou G D, Lian B, and Song Z D 2025 *Phys. Rev. B* **111** 035110
[85] Shi H, Miao W, and Dai X 2025 *Phys. Rev. B* **111** 155126
[86] Wang Y J, Zhou G D, Peng S Y, Lian B, and Song Z D 2024 *Phys. Rev. Lett.* **133** 146001
[87] Youn S, Goh B, Zhou G D, Song Z D, and Lee S S B 2024 arXiv: 2412.03108 [cond-mat.str-el]
[88] Parker D E, Soejima T, Hauschild J, Zaletel M P, and Bultinck N 2021 *Phys. Rev. Lett.* **127** 027601
[89] Wagner G, Kwan Y H, Bultinck N, Simon S H, and Parameswaran S A 2022 *Phys. Rev. Lett.* **128** 156401
[90] Wang Y J, Zhou G D, Jung H, Youn S, Lee S S B, and Song Z D 2026 arXiv: 2601.16525 [cond-mat.str-el]
[91] See Supplemental Material for detailed information on quantum impurity model, spectral function and correlation selfenergy *ansätze*, effective interactions, and NRG verification, which also includes Ref. [102,131–146].
[92] Andrei N, Furuya K, and Lowenstein J H 1983 *Rev. Mod. Phys.* **55** 331
[93] Parcollet O, Georges A, Kotliar G, and Sengupta A 1998 *Phys. Rev. B* **58** 3794
[94] Nozières P and Blandin A 1980 *J. Phys.* **41** 193
[95] Hewson A C 1993 *J. Phys.: Condens. Matter* **5** 6277
[96] Hewson A C 1993 *Phys. Rev. Lett.* **70** 4007
[97] Hewson A C, Oguri A, and Meyer D 2004 *Eur. Phys. J. B* **40** 177
[98] Nishikawa Y, Crow D J G, and Hewson A C 2010 *Phys. Rev. B* **82** 115123
[99] Yamada K 1975 *Prog. Theor. Phys.* **53** 970
[100] Yamada K 1975 *Prog. Theor. Phys.* **54** 316
[101] Yoshimori A 1976 *Prog. Theor. Phys.* **55** 67
[102] Georges A, Kotliar G, Krauth W, and Rozenberg M J 1996 *Rev. Mod. Phys.* **68** 13
[103] von Delft J, Zaránd G, and Fabrizio M 1998 *Phys. Rev. Lett.* **81** 196
[104] Krishnan A and Metlitski M A 2024 arXiv: 2408.12650 [cond-mat.str-el]
[105] Toulouse G 1969 *C. R. Acad. Sci.* **268** 1200
[106] Emery V J and Kivelson S 1992 *Phys. Rev. B* **46** 10812
[107] Kotliar G and Si Q 1996 *Phys. Rev. B* **53** 12373
[108] von Delft J and Schoeller H 1998 *Ann. Phys.* **510** 225
[109] Zaránd G and von Delft J 2000 *Phys. Rev. B* **61** 6918
[110] Giamarchi T 2003 *Quantum Physics in One Dimension* (Vol. 121) (Clarendon Press)
[111] Schiller A and De Leo L 2008 *Phys. Rev. B* **77** 075114
[112] Yuval G and Anderson P W 1970 *Phys. Rev. B* **1** 1522
[113] Anderson P W, Yuval G, and Hamann D R 1970 *Phys. Rev. B* **1** 4464
[114] Nishikawa Y, Crow D J G, and Hewson A C 2012 *Phys. Rev. Lett.* **108** 056402
[115] Costi T A 2000 *Phys. Rev. Lett.* **85** 1504
[116] Bulla R, Costi T A, and Pruschke T 2008 *Rev. Mod. Phys.* **80** 395
[117] Moca C P, Chirla R, Dóra B, and Zaránd G 2019 *Phys. Rev. Lett.* **123** 136803
[118] Fabrizio M, Ho A F, Leo L D, and Santoro G E 2003 *Phys. Rev. Lett.* **91** 246402
[119] Leo L D and Fabrizio M 2004 *Phys. Rev. B* **69** 245114
[120] Jayaprakash C, Krishna-murthy H R, and Wilkins J W 1981 *Phys. Rev. Lett.* **47** 737
[121] Jones B A and Varma C M 1987 *Phys. Rev. Lett.* **58** 843
[122] Jones B A, Varma C M, and Wilkins J W 1988 *Phys. Rev. Lett.* **61** 125
[123] Jones B A and Varma C M 1989 *Phys. Rev. B* **40** 324
[124] Affleck I and Ludwig A W W 1992 *Phys. Rev. Lett.* **68** 1046
[125] Gan J 1995 *Phys. Rev. Lett.* **74** 2583
[126] Mitchell A K and Sela E 2012 *Phys. Rev. B* **85** 235127
[127] Mitchell A K, Sela E, and Logan D E 2012 *Phys. Rev. Lett.* **108** 086405
[128] Zhang Y H and Mao D 2020 *Phys. Rev. B* **101** 035122
[129] Zhao J Y, Zhou B, and Zhang Y H 2025 arXiv: 2507.00139 [cond-mat.str-el]
[130] Zhao J Y and Zhang Y H 2025 arXiv: 2510.26801[cond-mat.str-el]
[131] Lichtenstein A I and Katsnelson M I 1998 *Phys. Rev. B* **57** 6884

[132] Hu H, Song Z D, and Bernevig B A 2025 arXiv: 2502.14039 [cond-mat.str-el]
[133] Hubbard J 1964 *Proc. R. Soc. Lond. A* **277** 237
[134] Ledwith P J, Dong J, Vishwanath A, and Khalaf E 2025 *Phys. Rev. X* **15** 021087
[135] Zhao J Y, Zhou B, and Zhang Y H 2025 *Phys. Rev. B* **112** 085107
[136] Costi T A, Hewson A C, and Zlatic V 1994 *J. Phys.: Condens. Matter* **6** 2519
[137] Krishna-murthy H R, Wilkins JW, and Wilson K G 1980 *Phys. Rev. B* **21** 1003
[138] Lee S S B and Weichselbaum A 2016 *Phys. Rev. B* **94** 235127
[139] Lee S S B, von Delft J, and Weichselbaum A 2017 *Phys. Rev. Lett.* **119** 236402
[140] Weichselbaum A 2024 *SciPost Phys. Codebases* 40
[141] Weichselbaum A 2024 *SciPost Phys. Codebases* 40-r4.0
[142] Yoshida M, Whitaker M A, and Oliveira L N 1990 *Phys. Rev. B* **41** 9403
[143] Campo V L and Oliveira L N 2005 *Phys. Rev. B* **72** 104432
[144] Žitko R and Pruschke T 2009 *Phys. Rev. B* **79** 085106
[145] Galpin M R, Logan D E, and Krishnamurthy H R 2005 *Phys. Rev. Lett.* **94** 186406
[146] Krishna-murthy H, Wilkins J, and Wilson K 1980 *Phys. Rev. B* **21** 1044